HAL open science

Microstratigraphic reconstruction of formation processes and paleoenvironments at the Early Pleistocene Cornelia-Uitzoek hominin site, Free State Province, South Africa

Michael Toffolo, James Brink, Francesco Berna

▶ **To cite this version:**

Michael Toffolo, James Brink, Francesco Berna. Microstratigraphic reconstruction of formation processes and paleoenvironments at the Early Pleistocene Cornelia-Uitzoek hominin site, Free State Province, South Africa. Journal of Archaeological Science: Reports, 2019, 25, pp.25-39. 10.1016/j.jasrep.2019.03.033 . hal-02090808

HAL Id: hal-02090808

https://hal.science/hal-02090808v1

Submitted on 22 Oct 2021

HAL is a multi-disciplinary open access archive for the deposit and dissemination of scientific research documents, whether they are published or not. The documents may come from teaching and research institutions in France or abroad, or from public or private research centers.

L'archive ouverte pluridisciplinaire **HAL**, est destinée au dépôt et à la diffusion de documents scientifiques de niveau recherche, publiés ou non, émanant des établissements d'enseignement et de recherche français ou étrangers, des laboratoires publics ou privés.

Distributed under a Creative Commons Attribution - NonCommercial 4.0 International License

Version of Record: https://www.sciencedirect.com/science/article/pii/S2352409X1930015X
Manuscript_e5a4337eb3c2facc4c196cf9b59950d4

Microstratigraphic reconstruction of formation processes and paleoenvironments at the Early Pleistocene Cornelia-Uitzoek hominin site, Free State Province, South Africa

Michael B. Toffolo[a,b,*], James S. Brink[a,c], Francesco Berna[d]

[a]Florisbad Quaternary Research Department, National Museum, 36 Aliwal Street, Bloemfontein 9300, South Africa.

[b]Institut de Recherche sur les Archéomatériaux-Centre de Recherche en Physique Appliquée à l'Archéologie (IRAMAT-CRP2A), UMR 5060 CNRS, Université Bordeaux Montaigne, 8 Esplanade des Antilles, Pessac 33607, France.

[c]Centre for Environmental Management, University of the Free State, 205 Nelson Mandela Drive, Bloemfontein 9300, South Africa.

[d]Department of Archaeology, Simon Fraser University, 8888 University Drive, Burnaby BC V5A 1S6, Canada.

*Corresponding author. Phone: +33 (0)5 57 12 46 81. Email address: michael.toffolo@u-bordeaux-montaigne.fr

Abstract

The Cornelia-Uitzoek fossil site has produced a large collection of bones, Acheulean artifacts and a *Homo* sp. tooth dated to ~1 million years ago. The faunal assemblage defines the Cornelian Land Mammal Age and is characterized by a number of extinct species of large mammals that reflect an open grassland environment. Bones were accumulated by hyenas, whereas artifacts appear to be chance inclusions, although they suggest human presence in the immediate surroundings. Previous studies established the absolute chronology of the site and a broad stratigraphic sequence. However, the sedimentary units identified in the field were not linked to specific formation processes, thus limiting the understanding of the depositional history of the site and its potential in reconstructing Pleistocene environments. Using a microgeoarchaeological approach based on infrared spectroscopy and micromorphology of sediments, we were able to determine the formation and post-depositional processes of the entire stratigraphic sequence, and to show that the site is characterized by alluvial sediments accumulated under different river flow regimes. Our results provide context to the faunal and lithic assemblages and are in agreement with existing paleoenvironmental data for the site.

Keywords: paleoenvironment; micromorphology; FTIR; Cornelian; Acheulean; formation processes; South Africa

© 2019 published by Elsevier. This manuscript is made available under the CC BY NC user license
https://creativecommons.org/licenses/by-nc/4.0/

1 Introduction

Early Pleistocene open-air archaeological and fossil sites are rather rare occurrences in the central interior of South Africa, as they are confined to preserved "pockets" of sediments bearing artifacts and bones deposited in the shallow valleys of meandering rivers, such as the Vaal and its tributaries (e.g. Mason, 1961; Helgren, 1978; Li et al., 2017; Kuman and Gibbon, 2018). Considered their paucity, these sites are an exceptionally important source of information about hominin adaptation to open landscapes and changing environments, especially in a region located outside the Malmani dolomitic karst landscape that is home to the Cradle of Humankind, which produced a large number of fossils including hominin remains (Eriksson and Altermann, 1998; Kuman, 2016). Therefore, the characterization of paleoenvironments at these alluvial sites using sediments and bones as a proxy holds considerable value for our understanding of the evolution of early hominins in southern Africa.

One of these notable localities in the interior is Cornelia-Uitzoek, a Pleistocene fossil-bearing site near the town of Cornelia, in the Highveld plateau of the northeastern Free State Province of South Africa (henceforth Free State), at 1540 m a.s.l. (Figure 1). The site is the type locality of the Cornelian Land Mammal Age (LMA), a period between ~1.1 and 0.6 Ma characterized by a number of extinct species of large mammals that follows the Makapanian and precedes the Florisian LMAs (Cooke, 1974; Hendey, 1974; Lacruz et al., 2002; Brink, 2004; Brink et al., 2012). In addition, Cornelia-Uitzoek has produced a substantial assemblage of Acheulean artifacts and a *Homo* sp. tooth dated to ~1 Ma (Clark, 1974; Brink et al., 2012).

The most prominent faunal occurrence found at the site is a large bone bed located at the bottom of the sequence, which was dated to ~1 Ma using paleomagnetism (Brink et al., 2012). Bones make up the typical Cornelian assemblage dominated by open-grassland and water-dependent species and were accumulated by hyenas in a burrow, as suggested by the presence of coprolites and gnawing marks. The same locality yielded the largest concentration of Acheulean artifacts at the site, including handaxes and cleavers. At present there is no explicit link between bones and artifacts, which are interpreted as chance inclusions in the bone bed from an ancient land surface, based on their random occurrence throughout the deposit and on the absence of cutmarks on bones (Brink, 2004). It should be noted that the presence of all stages of the operational chain except for cores may indicate local finishing and use of bifaces (Brink et al., 2012).

The study of Brink et al. (2012) established a general stratigraphic sequence of the site by differentiating sediment types at the macroscopic scale. However, sedimentary features were not linked to specific formation processes, and as a result the depositional history of the site is not well

understood, especially in relation to faunal assemblages. Therefore, the present study is aimed at addressing outstanding questions regarding site formation processes, including how the latter can provide insights into changing paleoenvironments during the Early Pleistocene. To achieve this goal, we employed a microgeoarchaeological approach based on Fourier transform infrared spectroscopy (FTIR) and micromorphology of sediments, which address different aspects of the microscopic record (e.g. Goldberg and Berna, 2010; Weiner, 2010; Karkanas and Goldberg, 2019). More specifically, FTIR was used to differentiate clay minerals and determine the preservation state of bones, whereas micromorphology allowed the study of sediments at the microscopic scale and within their original depositional context. By doing so, we were able to identify microscopic sedimentary structures and components related to different regimes of alluvial deposition and post-depositional alteration, which are in agreement with other paleoenvironmental proxies, such as faunal assemblages and stable isotopes analysis of tooth enamel. In addition, our results support the interpretation of the bone bed formation proposed by Brink (2004), according to which hyenas burrowed an existing paleo-donga, and provide context to the local landscape in which early hominins lived.

2 Materials and methods

2.1 Site settings and sampling strategy

The Cornelia-Uitzoek occurrence was discovered and excavated in the 1920s by E. C. N. van Hoepen, who first described the stratigraphic sequence and faunal collection (van Hoepen, 1930, 1932b, a, 1947). Another excavation season led by A. C. Hoffman took place in 1953 (Clark, 1974), whereas K. W. Butzer later described the sedimentary context (Butzer, 1974). Surface collection of fossils was resumed in the early 1990s by J. S. Brink (Bender and Brink, 1992), who started a new excavation program in 1998 (Brink and Rossouw, 2000).

The latest investigations uncovered a large amount of faunal and lithic evidence, and determined its chronology and geomorphological context (Brink et al., 2012). The site is located within a pocket of alluvial clay and gravel deposits carved into the local Permian shale bedrock of the Ecca Group (Karoo Supergroup), a mudstone made of clay minerals and fine-grained quartz. Shale has been intruded in places by Jurassic dolerite, a mafic subvolcanic rock similar to basalt (see Toffolo et al., 2017 for a detailed mineralogical description). The alluvial sequence has been incised by the Schoonspruit River, a left-bank tributary of the Vaal River that flows in a northerly direction, about 50 m west of the site (Tooth et al., 2004). Geological and climatic constraints and the limited bedload of the Schoonspruit in recent times favored bank erosion, which determined the formation of deep erosional gullies, locally termed “dongas” (Figure 2 and Figures S1-S4). These

features exposed clusters of fossils and artifacts at different elevations within the stratigraphic sequence.

In this study we followed the stratigraphic sequence and sedimentary units established by Brink et al. (2012), which is summarized in Table 1. From bottom to top, the sequence features Ecca shale, Banded Gravel Bed (BGB; Figure 3), Mottled Yellow Clay (MYC; Figure 4), Laminated Orange Clay (LOC; Figure 5-6), Orange Coarse Gravel (OCG; Figure 7), Dark Grey Clay (DGC) and Black Turf Soil (BTS; Figure 8). The bone bed appears as a linear and horizontal intrusive feature (such as a burrow), about 2.5 m long, with limited vertical displacement of bones (50 cm) and a poorly consolidated sedimentary matrix compared to the surrounding MYC (Figure 4) (Brink, 2004: Figure 4). These features led Brink (2004) to propose that hyenas reused and burrowed an existing paleo-donga or similar erosional feature to make their lair.

In order to determine the formation processes that led to the accumulation of the deposits and to reconstruct paleoenvironments based on the sequence of different sedimentary environments, we opted for a microgeoarchaeological approach geared towards the identification of mineral components and diagnostic sedimentary structures (Goldberg and Berna, 2010; Karkanas and Goldberg, 2019). In particular, we used FTIR spectroscopy to characterize clay minerals and bones, and micromorphology of sediments to observe microstratigraphy and all the features and components that are not visible to the naked eye but contain valuable embedded information regarding depositional processes.

Sediment and bone samples were collected from freshly exposed sections of the bone bed (MYC unit) and different locales within the dongas in order to study the full stratigraphic sequence, which is not entirely represented in one single section (Figure 3-8). Depositional units were sampled at different locales and multiple bulk sediment samples were collected at random intervals to address lateral variability. However, at the macroscopic level sedimentary units appeared homogeneous over tens of meters and thousands of square meters in surface area. The DGC was not recognized as a separate sedimentary unit in the field and thus was not sampled. Bones were randomly selected from the bone bed collection curated at the Florisbad Research Station of the National Museum to study their degree of diagenesis. Samples were immediately analyzed at an on-site laboratory that included an infrared spectrometer and a petrographic microscope (Weiner, 2010). Preliminary information on mineral components and particle size was obtained with smear slides. A few milligrams of bulk sediment sample were mounted onto a glass slide using Entellan New (Merck) and analyzed at the on-site laboratory using a Nikon Optiphot petrographic microscope at different magnifications (20x, 50x, 100x, 200x, 400x).

2.2 Fourier transform infrared spectroscopy (FTIR)

Bulk sediment samples were collected using a stainless-steel spatula, placed in 40 ml plastic vials marked with progressive sample numbers, and their composition was determined at the site using FTIR spectroscopy. After return to the home laboratory at the Florisbad Research Station, bones were analyzed as well to determine their degree of preservation. A few milligrams of each sediment (*n*=57) and bone (*n*=15) sample were homogenized and powdered in an agate mortar and pestle. About 0.1 mg were left in the mortar, mixed with approximately 0.5 mg of KBr (FTIR grade, Sigma-Aldrich) and pressed into a 7-mm pellet using a hand press (PIKE Technologies). Infrared spectra were obtained at 4 cm^{-1} resolution in 32 scans within the 4000-400 cm^{-1} spectral range using a Thermo Fisher Scientific Nicolet ™ iS5 spectrometer. Phase identification was performed using OMNIC v. 9, standard literature (Farmer, 1974; van der Marel and Beutelspacher, 1976), and the reference collection of FTIR spectra of standard materials provided by the Kimmel Center for Archaeological Science, Weizmann Institute of Science (http://www.weizmann.ac.il/kimmel-arch/infrared-spectra-library).

2.3 Micromorphology of sediments

Micromorphology was used to study sediments within their original depositional context, in order to determine their formation and post-depositional processes. Boundaries between sedimentary units were selected to highlight changes in depositional environments. In addition, samples from the middle portion of the MYC unit and bone bed were collected to differentiate their contents. Intact blocks of sediment (*n*=11) were carved from sections, air-dried for several weeks and finally oven-dried at 40°C for three days. Samples were then embedded in a mixture of polyester resin (NCS General Purpose Polyester) and acetone (ratio 7:3), with the addition of 1.5 ml catalyst per liter of mixture. Hardened blocks were sliced with a rock saw to obtain 55x75 mm chips, which were shipped to Arizona Quality Thin Sections (Tucson, Arizona, USA) for thin section preparation. Two additional samples were prepared at the thin section laboratory of the University of Bordeaux (France). All the thin sections were polished to a thickness of 30 µm. Micromorphological analyses were carried out using Olympus BX41 and Leica DM2500 P petrographic microscopes at different magnifications (20x, 25x, 40x, 50x, 100x, 200x, 400x). Descriptions and interpretations are based on conventional criteria developed in the specialized literature (Courty et al., 1989; Delvigne, 1998; Stoops, 2003; Flügel, 2004; Goldberg and Macphail, 2006; Stoops et al., 2010; Macphail and Goldberg, 2017). We use here the concept of "microfacies" (MFT) as described by E. Flügel, i.e. "*the total of all sedimentological and paleontological data which can be described and classified from thin sections* […]" (Flügel, 2004: 1). This term defines discrete assemblages of sediment types

based on the information retrieved from the analysis of thin sections. Considered that some depositional units occur repeatedly throughout the stratigraphic sequence (e.g. MYC and LOC) and that multiple thin sections were obtained from these units, the use of MFTs allows rapid reporting of results. This approach to the study of thin sections includes the basic interpretive level of each MFT (e.g. Goldberg and Aldeias, 2018).

3 Results

The chemical phases identified with FTIR spectroscopy are displayed in Figure 8. Sedimentary components and structures observed in thin section are shown in Figure 9 and Figure 10; MFTs are listed in Table 2. Below follows a description of the stratigraphic sequence from bottom to top, based on the framework established by Brink et al. (2012). Micromorphological terminology by Stoops (2003) is noted in *italics* between brackets next to the explanation of the relative feature at its first appearance.

3.1 Bedrock and Banded Gravel Bed

The sedimentary sequence rests on top of Ecca shale. An unconformity separates bedrock from the BGB (Figure 3), a layer of gravel characterized by normal graded bedding and dated to the Matuyama reversal (>1.07 Ma). The coarse components (mainly cobbles to very fine pebbles with a few boulders at the base) are mostly fragments of Ecca shale and Jurassic dolerite and they are supported by a clayey matrix towards the top. Cross bedding is visible in places.

3.2 Mottled Yellow Clay and Laminated Orange Clay

The next unit in the sequence is the MYC (Figure 4), a layer of massive pale-yellow to pale-green clay (depending on moisture), dated to the Jaramillo subchron (1.07-0.99 Ma). This deposit includes the hyena bone bed that yielded a rich assemblage of Cornelian-age fossils, a human tooth, and Acheulean artifacts (Brink, 2004). The sedimentary matrix of this layer comprises a mixture of clay minerals of the smectite (dominant) and kaolinite (minor) groups, as indicated by the absorptions at 3690, 3620, 1090, 1032 and 525 cm^{-1}, and a minor amount of quartz (absorptions at 797, 779, 694 and 470 cm^{-1}) and feldspars (absorption at 646 cm^{-1}). Yellow mottles exhibit stronger absorptions of kaolinite clays at 3697, 3620, 1009, 911, 791, 750, 670 and 536 cm^{-1} (Figure 9). Black clay nodules rich in manganese oxides occur in places (broad absorption at 3405 cm^{-1}). Bones are characterized by the occurrence of fluoridated carbonate hydroxyapatite on the outer surface of cortical tissue (absorption at 604 cm^{-1} higher than the absorption at 567 cm^{-1}; Figure 9) (Geiger and Weiner, 1993).

Observed in thin section, the MYC shows the characteristic features of the "clay" MFT (Table 2), which exhibits a dominant fraction of silt-sized grains of quartz and feldspar embedded in a pale-green clay (*porphyric c/f related distribution*). Coarser sand-sized grains occur frequently, thus making the coarse fraction poorly to moderately sorted. Porosity is represented by thin, elongated voids that separate angular blocks of sediment (*angular blocky microstructure* with *planes*), with a few cylindrical, elongated voids (*channels*). Below the level of the bone bed, the fabric of the coarse fraction appears to be oriented horizontally in places due to bedding; fragmented, horizontal silty-clay crusts showing normal graded bedding occur as well (Figure 10a-b). No bedding was observed within the bone bed fill, and a substantial proportion of rounded, very fine pebbles (2-4 mm) of shale make up the coarse fraction together with poorly sorted quartz sand/silt (Figure 10c). The poor degree of compaction of shale pellets determines the occurrence of voids resulting from loose packing (*simple packing voids*) and in general of greater porosity compared to lower levels. Throughout the entire layer, the fine fraction is characterized by domains of clay minerals oriented in small patches, along random straight lines, or around grains and pores, as evidenced by their birefringence fabric (*stipple speckled, striated, granostriated and porostriated b-fabric*, respectively; Figure 10d). Post-depositional processes (*pedofeatures*) are represented mainly by the translocation of clays through groundwater movement. Two distinct events were observed: dense accumulations of clay in pores (*intercalations*) and void coatings composed of dark-green clay; laminated void coatings and dense void infillings of yellow clay, often juxtaposed to the dark-green clay features (Figure 10e-f). In addition, different types of Fe-Mn oxide aggregate nodules are superimposed on the fine fraction, shale fragments and clay coatings/infillings (Figure 10g). Reddish Fe-Mn oxide halos around pores (*hypocoatings* and *quasicoatings*) occur as well (Figure 10h).

A sharp erosive boundary separates the MYC from the LOC (Figure 5-6), a layer composed of alternated beds of clay and fine gravel and dated to the Matuyama reversal (0.99-0.78 Ma). Clay beds exhibit the same FTIR spectra as the MYC, with black patches of Fe-Mn oxides and yellow mottles richer in kaolinite minerals, whereas gravel is composed of rounded fine pebbles of local Ecca shale. Bones exhibit absorptions of fluoridated carbonate hydroxyapatite.

Clay beds show the microscopic characteristics of the "clay" MFT (Table 2). In addition to the features observed in the MYC, the LOC clay beds exhibit cm-deep bands of diffuse Fe oxide halos (*impregnations*) (Figure 11a), close to the boundary with the overlying layer. These bands are superimposed on the fine fabric (*groundmass*) and represent ancient surface zones of enhanced Fe oxidation, favored by a concentration of plant material and microorganisms in a fluctuating water table, possibly in relation to river floods (Courty et al., 1989; Lindbo et al., 2010). A similar process

occurred in the case of dense void infillings composed of silt embedded in red clay (Figure 11b). These pedofeatures are related to the presence of root casts of woody and/or herbaceous plants, a common occurrence at the site (Figure 12). These vertical channels are pseudomorphs of roots derived from ancient surfaces and were observed throughout the entire sedimentary sequence, except for topsoil. The decay of plant material due to microorganism activity favors the mobilization of Fe and its subsequent precipitation due to exposure to air in the channel left by the root (Lindbo et al., 2010). This is later infilled by coarse sediment from the overlying layer. Furthermore, clay beds are characterized by a greater proportion of Fe-Mn oxide aggregate nodules.

Gravel beds show the characteristic features of the "fine gravel" MFT (Table 2). Coarse fraction is composed of shale pebbles (very fine to medium) linked by clay bridges that often coat grains (*chitonic* to *concave gefuric c/f related distribution*), whereas fine fraction is rarely present (Figure 11c). Pores derive from the spatial arrangement between pebbles and from their degree of compaction (*weakly separated granular microstructure* to *vughy microstructure* with *compound packing voids*, *regular vughs* and *star-shaped vughs*). Similar to previous sedimentary units, the LOC exhibits juxtaposed dark-green and yellow clay coatings with superimposed Fe-Mn aggregate nodules (Figure 11d).

3.3 Orange Coarse Gravel and Black Turf Soil

Another sharp, wavy and erosive boundary, which corresponds to the beginning of the Brunhes chron (<0.78 Ma), marks the transition between the LOC and the OCG (Figure 7). Clasts are medium to very coarse pebbles and show different fabric depending on the location within the layer. Cross-bedding and imbrication are visible in places, especially in the lower portion of the unit.

The chemical composition of the fine fraction is comparable with the MYC and LOC, showing a mixture of kaolinite (dominant) and smectite clay minerals (Figure 9). Bones were not found in this sedimentary unit. A number of cm-size nodules coated with a black film exhibit absorption bands of kaolinite and Fe-Mn oxides. These components are concentrated at the transition with the overlying topsoil and can be observed today at the top of the donga as a lag product of the erosion of finer topsoil material (Figure 13).

The microscopic features of the OCG can be grouped under the "coarse gravel" MFT (Table 2), which presents similarities with the "clay" MFT. More specifically, the poorly sorted coarse fraction is embedded in yellow clay (*porphyric c/f related distribution*) and is characterized by planes (*angular blocky microstructure*); the fine fraction exhibits prominent striated, porostriated

and granostriated b-fabrics. However, there are also notable differences, namely the greater proportion of coarse particles, the occurrence of considerable amounts of dolerite pebbles (Figure 11e) and Fe-Mn oxide typic nodules, and the absence of intrusive pedofeatures, such as clay coatings. Oxide nodules are mainly round and exhibit sharp boundaries, implying that they formed elsewhere within the OCG before reaching their final location (*disorthic nodules*). Other nodules instead clearly formed in situ (*orthic nodules*), as suggested by their irregular boundary or concentric appearance (Figure 11f-g).

The OCG grades into the BTS (Figure 8), a soil profile characterized by an orthic A horizon (Soil Classification Working Group, 1991). As stated, the transition boundary exhibits a large number of 0.5-1 cm round pellets composed of Fe-Mn oxides. In places, especially at the top of dongas and close to the erosion line, the BTS plant cover has disappeared, thus exposing soil horizon to rain, erosion, and oxidation of organic compounds. The latter favored a change in color from brown to dark grey, hence the thin Dark Grey Clay (DGC) layer reported by Brink et al. (2012) as patches in between the OCG and BTS (Figure 14). In addition, the DGC layer is characterized by large accumulations of Fe-Mn oxide pellets left behind as lag deposit after the erosion of fine material. Therefore, the DGC appears to be a weathering product of the BTS and thus its description coincides with the latter.

Looking at FTIR spectra, the BTS sediments are composed of a mixture of kaolinite (dominant) and smectite clay minerals, quartz and feldspars. Compared to the MYC and LOC, they contain a larger proportion of kaolinite minerals. The microscopic features of this sedimentary unit are ascribed to the “topsoil” MFT (Table 2) and comprise a poorly sorted coarse fraction (quartz silt and sand) embedded in a dark-brown clay with undifferentiated b-fabric and large amounts of amorphous organic matter. Plant fibers occur as well and are part of the current vegetal cover. Porosity is almost absent and confined to a few channels created by plant roots in an otherwise massive microstructure. The latter is disrupted by extensive areas of intense bioturbation, as indicated by the presence of *Oribatida* mites excrements (Figure 11h) (Kooistra and Pulleman, 2010). Besides faunal activity, pedofeatures include typic orthic and disorthic nodules of Fe-Mn oxides, especially close to the boundary with OCG.

4 Discussion

The results of FTIR and micromorphological analyses presented herein allow the interpretation of the stratigraphic sequence in relation to archaeological, faunal, geologic and environmental evidence previously published for the site and the region.

4.1 Formation and post-depositional processes

Starting from the bottom, it appears that the unconformity between bedrock and BGB may account for multiple cycles of sedimentation and erosion that took place between the Permian and Early Pleistocene, a common feature in southern African sedimentary contexts, including the Free State (e.g. Loock and Grobler, 1988; Toffolo et al., 2017). Based on the large clast size (up to boulders), the BGB is a point bar or channel deposit accumulated under high-energy water conditions consistent with a braided river system, perhaps the paleo-Schoonspruit, whose catchment basin drained an area characterized by local Karoo-aged lithology.

Further up in the sequence, the localized horizontal fabric of the coarse fraction and the presence of clay crusts lend support to the interpretation of the MYC as an overbank deposit in a meandering paleo-Schoonspruit, characterized by low-energy water; in particular, clay crusts represent remnants of ancient depositional surfaces (Courty et al., 1989; Vingiani et al., 2018). Instead, the bone bed fill shows no layering and a greater proportion of pores (low compaction) and coarse components, including rounded, very fine pebbles of shale and poorly sorted quartz. These features are consistent with a chaotic accumulation of sediment as infill of a "pocket" within the MYC, which might be the result of hyena burrowing and bone concentration, and colluvium deposition as observed in present-day donga channels (Figure 15). Micromorphological observations thus seem to support the interpretation advanced by Brink (2004) and Brink et al. (2012) regarding the location of the hyena den within a paleo-donga or channel created by localized erosion in the vicinity of the river.

Bones appear to be well preserved, and this is confirmed by the occurrence of fluoridated carbonate hydroxyapatite. This mineral is known to form in extremely old fossils (e.g. Piga et al., 2011) and in more recent bones exposed to fluoride-rich groundwater (e.g. Toffolo et al., 2015) due to the replacement of OH^- ions with F^- ions in more symmetrical locations within the crystal lattice of carbonate hydroxyapatite. As a result, bone mineral becomes more resistant to chemical weathering (Newesely, 1989; LeGeros, 1991). Based on their good state of preservation from both the morphological and chemical point of view, bones must have been exposed on the surface only briefly, and the bone bed buried rather quickly by overlying sediments.

In addition, several post-depositional processes considerably affected the MYC. First, the striated b-fabric and angular blocky microstructure are typical of shrink/swell processes in smectites (Courty et al., 1989), which were identified with FTIR, and are consistent with a pronounced vertic behavior of sediments (Toffolo and Berna, 2008; Kovda and Mermut, 2010). These processes likely contributed to the slight slumping and fragmentation of some bone specimens observed by Brink

(2004). Second, pores are often coated/filled with dark-green clay and yellow clay. The former is the result of fine illuviation from a vegetated topsoil, now lost, that developed on the MYC layer, whereas the latter may be ascribed to several episodes of fine illuviation (based on the laminated appearance of the coatings) from overlying layers (Courty et al., 1989), e.g. the OCG; according to FTIR, yellow clay mottles include a larger proportion of kaolinite minerals compared to the general sedimentary matrix, and that is the main component of clay minerals in the OCG. Third, the presence of Fe-Mn redoximorphic features in the form of coatings and nodules juxtaposed or superimposed on coarse and fine components points to periodic waterlogging of sediments (Courty et al., 1989). Fe and Mn ions are mobilized under waterlogged conditions and subsequently oxidize upon drying, creating aggregate nodules and hypo- and quasi-coatings of pores (Lindbo et al., 2010). The antiquity of these pedofeatures is demonstrated by the occurrence of yellow clay coatings in voids characterized by Fe-Mn oxide hypo-coatings (Figure 10h). In addition, the fact that bones exhibit Mn staining and patches of fluoridated carbonate hydroxyapatite indicates they were exposed for prolonged periods to groundwater rich in both elements.

The MYC and LOC appear to be the product of similar formation and post-depositional processes. The thick layer of MYC was deposited as overbank during floods and provided the surface where hyenas dug their lair and accumulated carcasses. The same land surface was likely characterized by human presence and possibly sporadic occupation; the occurrence of Acheulean handaxes and cleavers together with flakes and blanks suggests that artifacts were produced close to the site (Brink et al., 2012). Their inclusion in the bone bed fill could be due to deliberate discard, or it might be the result of the burrowing activity of hyenas and later colluvium in the paleo-donga channel. In the absence of clear occupation surfaces, the latter hypothesis seems the most likely based on micromorphological data. However, this does not rule out the possibility that humans roamed the site (as indicated by the tooth). The erosive contact with the overlying LOC, which corresponds to a stripped land surface from which the dark-green clay translocated downwards into voids, marks a change in the depositional pattern, with clay beds similar to the MYC that alternate with fine gravel beds accumulated under conditions of slightly higher-energy water. As observed in the field, where multiple bone scatters were recorded at different levels within the LOC, each of the clay and fine gravel beds provided temporary land surfaces that functioned as accumulation sites for bones and artifacts, although not in the same proportions as in the hyena bone bed. Given the small size of these bone assemblages and the cyclic sedimentary pattern, it appears that hyenas were not the primary depositional agent of bones in the LOC. The presence of Fe oxide bands and root casts seems to support the occurrence of stable vegetated surfaces at different stages in the formation of the sedimentary unit, which would have encouraged human settlement of the area.

The large amount of pebble-sized clasts and the presence of cross-bedding and imbrication indicate that the OCG was deposited by high-energy water in a point bar or straight channel of a meandering river system (Courty et al., 1989). After deposition, this sedimentary unit underwent shrink/swell processes, represented by the prominent striated b-fabric. In addition, a large portion of the yellow clay that makes up the fine fraction translocated into the LOC and MYC through eluviation processes, thus creating the yellow clay coatings and infillings observed in lower units. In fact, the OCG is today the least visible sedimentary unit at the donga, due to its lower resistance to weathering. Its dissolution promoted the accumulation of a thin layer of shale clasts and Fe-Mn oxide nodules, which were left behind as lag deposit.

One last episode of alluvial deposition in conditions of low-energy water promoted the formation of the BTS. In addition, the presence of medium and coarse sand rounded grains of quartz points to an eolian component of the coarse fraction. This is a common characteristic at terminal Pleistocene-Holocene sites in the Free State (e.g. Lyons et al., 2014; Toffolo et al., 2017). This sedimentary unit lacks secure chronological pegs but considering the occurrence of sporadic Middle Stone Age artifacts and the almost completely reworked nature of the sediments, it seems that the age of this layer may well exceed 50 ka.

4.2 Paleoenvironments

Given the scarcity of paleo-climatic data for the Free State before 500 ka (e.g. deMenocal, 2004; Scott and Neumann, 2018), it is difficult to draw interpretations in that sense based solely on the sedimentary context. In addition, river flow in this region has been shown to be primarily affected by the erosion and retreat of dolerite knickpoints, which determine the slope and degree of sinuosity of riverbeds, rather than climate. The retreat of knickpoints ultimately depends on base level fall rates of the Vaal, which in the Plio-Pleistocene were governed by a complex mix of tectonic uplift and climate change at the regional level (Tooth et al., 2004 and references therein). However, recent paleoenvironmental data for the Limpopo River catchment basin, located to the immediate northeast of the Free State, show an increase in aridity after 1 Ma (Caley et al., 2018). Therefore, assuming wetter conditions before this threshold, which may have implied an increased flow regime of the Vaal and other rivers in the region and thus faster riverbed incision, it would seem that the BGB and the erosional hiatus with the overlying MYC were formed as a result of knickpoint retreat and larger water supply at the source. More detailed sedimentary and climatic data for this period in the northeastern Free State is nevertheless required in order to support this suggestion.

The occurrence in the bone bed of ungulates and water-dependent species, such as *Hippopotamus gorgops* (giant hippo) and *Syncerus antiquus* (giant long-horned buffalo) (Brink,

2004; Brink et al., 2012), together with the low-energy water environment characteristic of meandering rivers, suggest that the MYC represents a grassland landscape characterized by surface waters (i.e. oxbows, backwaters and swamps), similar to what is observed today in the upper reach of the Klip River in the Memel Seekoeivlei Nature Reserve, located about 70 km east of Cornelia. There, in areas characterized by soft sandstone bedrock away from dolerite outcrops and knickpoints, the river meanders within a large valley, creating oxbows and backswamps during summer rains (Tooth et al., 2002). This kind of environment probably developed also in the broad shale valley of the paleo-Schoonspruit around Cornelia-Uitzoek, thus attracting herbivores and with them carnivores and humans. Therefore, sedimentary and faunal evidence show that during the Early Pleistocene the central interior of South Africa offered a lush habitat favorable to human settlement, besides the well-known Malmani dolomitic karst. A later parallel in terms of grassland paleoenvironment with plenty of water is represented by Florisbad, in the mid-western Free State (e.g. Brink, 1987, 1988; Kuman et al., 1999; Brink and Henderson, 2001; Toffolo et al., 2017).

The formation of pedofeatures caused by shrink-swell episodes during the Pleistocene (i.e. dark-green clay coatings juxtaposed to subsequent yellow clay coatings originated from younger units), lends support to the hypothesis of the existence of a summer rainfall regime already at that time. Prolonged periods of drought during winter months and rainfall concentrated in summer may account for the presence of shrink/swell features. The possible existence of a paleo-donga, as suggested by thin sections, would also be a product of seasonal rains. This scenario seems in agreement with faunal data. Several individuals from the bone bed exhibit enamel $\delta^{13}C$ values >0‰, which are characteristic of a diet based on C_4 grasses, and diagnostic phytoliths from these plants were recovered from the same context (Codron et al., 2008). Plants that produce energy through C_4 processes typically grow in environments where groundwater is scarcely available due to high evapotranspiration, and this is a common trait of the Highveld grasslands especially during winter, the dry season (Mucina and Rutherford, 2006). The Limpopo paleoenvironmental dataset shows an increase in aridity after 1 Ma that may support the evidence from sediments, fauna and phytoliths (Caley et al., 2018).

This C_4 grassland environment persisted in the LOC, as evidenced by the low-energy water deposition of clay and fine gravel beds with multiple bone scatters of Cornelian age, and by root casts indicative of ancient land surfaces. However, the sharp boundary with the MYC might represent a relatively brief period of high-energy water erosion that removed the original land surface. A similar process likely stripped the latest land surface of the LOC and subsequently deposited the OCG. As mentioned for the meandering river, the deposition of coarse gravel might be a result of knickpoint exposure further upstream, which caused an increase in slope, a decrease

in sinuosity, and thus a more rapid flow able to transport coarser clasts (Tooth et al., 2004). The presence of dolerite pebbles in the OCG and not in sedimentary units above and below seems to support this interpretation, as these components would derive from the erosion of exposed dolerite. In addition, the regional trend towards increased aridity after 1 Ma (Caley et al., 2018) seems to exclude higher flow regime from the source as a possible cause for increased water energy and coarser sediment supply. The absence of faunal material in the OCG and the lack of data from other proxies (e.g. phytoliths, pollen) hinder a proper reconstruction of the paleoenvironment at this stage. Nevertheless, the occurrence of younger Acheulean artifacts towards the top of the OCG (Brink et al., 2012), perhaps transported by water, indicates that humans were present in the area. Additionally, the persistence of C_4 grasslands in the Highveld from the Cornelian through to the Florisian LMA as shown by faunal evidence (e.g. Brink, 1987, 1988; Lacruz et al., 2002; Brink, 2004; Codron et al., 2008; Brink et al., 2012; Brink et al., 2015; Brink, 2016), suggests that this kind of environment existed also at the time of deposition of the OCG. This is further confirmed by the fine alluvium altered by pedogenesis that makes up the BTS, the last layer deposited by the paleo-Schoonspruit during a meandering stage similar to previous ones, before the beginning of its current incising phase in the study area.

5 Conclusions

Cornelia-Uitzoek is the type locality of the Cornelian LMA (~1.1-0.6 Ma) and has produced a large faunal assemblage dated to ~1.0 Ma that is the result of bone accumulation by hyenas. In addition, the occurrence of a human tooth and several Acheulean artifacts indicates that hominins occupied the area around the site. This important paleoecological occurrence offered the opportunity to study in depth the environments in which humans lived, in a region that features an extremely limited number of human fossils. Using a microgeoarchaeological approach based on FTIR spectroscopy and micromorphology of sediments, we were able to identify mineral phases and microscopic sedimentary structures typical of deposition by low- and high-energy water, and thus we could determine the formation and post-depositional processes of the entire stratigraphic sequence, including the bone bed that yielded the faunal and lithic assemblages. What emerged is an alluvial environment dominated by local geology, which determined the amount and type of sediment supply. Phases of low-energy water deposition in a meandering river system were conducive to the formation of oxbows and backswamps that supported populations of large- to small-sized ungulates, as well as carnivores and humans. Instead, high-energy water led to erosional hiatuses in the stratigraphy and to the deposition of coarse material, bearing little or no faunal/lithic evidence. Increasing aridity as seen at a regional level in southeastern Africa and locally based on the presence of post-depositional shrink/swell and redoximorphic features, faunal assemblages and

stable isotopes datasets, points to C_4 grasslands as the dominant biome, which later expanded in the Florisian LMA. Faunal and sedimentary evidence highlight the role of the central interior of South Africa as favorable habitat for the evolution of early hominins, and the importance of addressing site-formation and post-depositional processes by looking also at the microscopic record.

Acknowledgements

This research project was conducted under the auspices of the National Museum, Bloemfontein, and funded by a NRF African Origins Platform Grant to James Brink (grant n. 82603), by a grant from the University of the Witwatersrand DST/NRF Centre of Excellence in Paleosciences (CoE-Pal) to James Brink (grant n. OP2015/25JB), by a grant from the Social Science and Humanity Research Council of Canada to Francesco Berna (grant n. 430-2013-000546), and by the National Museum, Bloemfontein. The authors wish to thank Nico Avenant, Britt Bousman, Daryl Codron, Sharon Holt, Liora Kolska Horwitz, Lloyd Rossouw, Louis Scott, Maitland Seaman, Jaco Smith, Cornie van Huyssteen, the staff of the Florisbad Research Station and the administration of the National Museum for their continued support during fieldwork and laboratory analyses. The authors would like to thank in particular Frederick Roelofse for granting permission to use a rock saw at the Department of Geology, University of the Free State. Michael Toffolo and James Brink are members of the research group "Bloemfontein Palaeosystems Centre". Michael Toffolo is supported by a grant from IdEx Bordeaux (grant n. ANR-10-IDEX-03-02). Finally, the authors wish to thank the reviewers for their insightful comments.

References

Bender, P.A., Brink, J.S., 1992. A preliminary report on new large mammal fossil finds from the Cornelia-Uitzoek site, South African Journal of Science 88, 512-515.

Brink, J.S., 1987. The archaeozoology of Florisbad, Orange Free State, Memoirs van die Nasionale Museum, Bloemfontein 24, 1-151.

Brink, J.S., 1988. The taphonomy and palaeoecology of the Florisbad spring fauna, Palaeoecology of Africa and the Surrounding Islands 19, 169-179.

Brink, J.S., Rossouw, L., 2000. New trial excavations at the Cornelia-Uitzoek type locality, Navorsinge van die Nasionale Museum Bloemfontein 16, 141-156.

Brink, J.S., Henderson, Z.L., 2001. A high-resolution Last Interglacial MSA horizon at Florisbad in the context of other open-air occurrences in the central interior of southern Africa: an interim statement, in: Conard, N.J. (Ed.), Settlement dynamics of the Middle Paleolithic and Middle Stone Age, Kerns Verlag, Tübingen, pp. 1-20.

Brink, J.S., 2004. The taphonomy of an Early/Middle Pleistocene hyaena burrow at Cornelia-Uitzoek, South Africa, Revue de Paléobiologie 23, 731-740.

Brink, J.S., Herries, A.I.R., Moggi-Cecchi, J., Gowlett, J.A.J., Bousman, C.B., Hancox, J.P., Grün, R., Eisenmann, V., Adams, J.W., Rossouw, L., 2012. First hominine remains from a ~1.0 million year old bone bed at Cornelia-Uitzoek, Free State Province, South Africa, Journal of Human Evolution 63, 527-535.

Brink, J.S., Bousman, C.B., Grün, R., 2015. A reconstruction of the skull of *Megalotragus priscus* (Broom, 1909), based on a find from Erfkroon, Modder River, South Africa, with notes on the chronology and biogeography of the species, Palaeoecology of Africa 33, 71-94.

Brink, J.S., 2016. Faunal evidence for a mid- and late Quaternary environmental change in southern Africa, in: Knight, J., Grab, S.W. (Eds.), Quaternary environmental change in southern Africa: physical and human dimensions, Cambridge University Press, Cambridge.

Butzer, K.W., 1974. Geology of the Cornelia Beds, Memoirs van die Nasionale Museum, Bloemfontein 9, 7-32.

Caley, T., Extier, T., Collins, J.A., Schefuß, E., Dupont, L., Malaizé, B., Rossignol, L., Souron, A., McClymont, E.L., Jimenez-Espejo, F.J., García-Comas, C., Eynaud, F., Martinez, P., Roche, D.M., Jorry, S.J., Charlier, K., Wary, M., Gourves, P.-Y., Billy, I., Giraudeau, J., 2018. A two-million-year-long hydroclimatic context for hominin evolution in southeastern Africa, Nature 560, 76-79.

Clark, J.D., 1974. The stone artefacts from Cornelia, O.F.S., South Africa, Memoirs van die Nasionale Museum, Bloemfontein 9, 33-62.

Codron, D., Brink, J.S., Rossouw, L., Clauss, M., 2008. The evolution of ecological specialization in southern African ungulates: competition- or physical environmental turnover?, Oikos 117, 344-353.

Cooke, H.B.S., 1974. The fossil mammals of Cornelia, O.F.S., South Africa, Memoirs van die Nasionale Museum, Bloemfontein 9, 63-84.

Courty, M.A., Goldberg, P., Macphail, R.I., 1989. Soils and Micromorphology in Archaeology, Cambridge University Press, Cambridge.

Delvigne, J.E., 1998. Atlas of micromorphology of mineral alteration and weathering, Mineralogical Association of Canada, Ottawa.

deMenocal, P.B., 2004. African climate change and faunal evolution during the Pliocene-Pleistocene, Earth and Planetary Science Letters 220, 3-24.

Eriksson, P.G., Altermann, W., 1998. An overview of the geology of the Transvaal Supergroup dolomites (South Africa), Environmental Geology 36, 179-188.

Farmer, V.C., 1974. The Infrared Spectra of Minerals, Mineralogical Society, London.

Flügel, E., 2004. Microfacies of carbonate rocks: Analysis, interpretation and application, Springer, Berlin.

Geiger, S.B., Weiner, S., 1993. Fluoridated carbonatoapatite in the intermediate layer between glass ionomer and dentin, Dental Materials 9, 33-36.

Goldberg, P., Macphail, R.I., 2006. Practical and Theoretical Geoarchaeology, Blackwell Publishing, Malden, MA.

Goldberg, P., Berna, F., 2010. Micromorphology and context, Quaternary International 214, 56-62.

Goldberg, P., Aldeias, V., 2018. Why does (archaeological) micromorphology have such little traction in (geo)archaeology?, Archaeological and Anthropological Sciences 10, 269-278.

Helgren, D.M., 1978. Acheulian settlement along the lower Vaal River, South Africa, Journal of Archaeological Science 5, 39-60.

Hendey, Q.B., 1974. The Late Cenozoic Carnivora of the South-Western Cape Province, Annals of the South African Museum 63, 1-369.

Karkanas, P., Goldberg, P., 2019. Reconstructing Archaeological Sites: Understanding the Geoarchaeological Matrix, Wiley Blackwell.

Kooistra, M.J., Pulleman, M.M., 2010. Features Related to Faunal Activity, in: Stoops, G., Marcelino, V., Mees, F. (Eds.), Interpretation of micromorphological features of soils and regoliths, Elsevier, Amsterdam, pp. 397-418.

Kovda, I., Mermut, A.R., 2010. Vertic Features, in: Stoops, G., Marcelino, V., Mees, F. (Eds.), Interpretation of micromorphological features of soil and regoliths, Elsevier, Amsterdam, pp. 109-127.

Kuman, K., Inbar, M., Clarke, R.J., 1999. Palaeoenvironments and Cultural Sequence of the Florisbad Middle Stone Age Hominid Site, South Africa, Journal of Archaeological Science 26, 1409-1425.

Kuman, K., 2016. Development of the archaeological record in southern Africa during the Earlier Stone Age, in: Knight, J., Grab, S. (Eds.), Quaternary Environmental Change in Southern Africa: Physical and Human Dimensions, Cambridge University Press, Cambridge, pp. 349-370.

Kuman, K., Gibbon, R.J., 2018. The Rietputs 15 site and Early Acheulean in South Africa, Quaternary International 480, 4-15.

Lacruz, R., Brink, J.S., Hancox, P.J., Skinner, A.R., Herries, A.I.R., Schmid, P., Berger, L.R., 2002. Palaeontology and geological context of a Middle Pleistocene faunal assemblage from the Gladysvale Cave, South Africa, Palaeontologia Africana 38, 99-114.

LeGeros, R.Z., 1991. Calcium Phosphates in Oral Biology and Medicine, Karger, Basel, Switzerland.

Li, H., Kuman, K., Lotter, M.G., Leader, G.M., Gibbon, R.J., 2017. The Victoria West: earliest prepared core technology in the Acheulean at Canteen Kopje and implications for the cognitive evolution of early hominids, Royal Society Open Science 4, 170288.

Lindbo, D.L., Stolt, M.H., Vepraskas, M.J., 2010. Redoximorphic Features, in: Stoops, G., Marcelino, V., Mees, F. (Eds.), Interpretation of micromorphological features of soils and regoliths, Elsevier, Amsterdam, pp. 129-147.

Loock, J.C., Grobler, N.J., 1988. The regional geology of Florisbad, Navorsinge van die Nasionale Museum Bloemfontein 5, 489-497.

Lyons, R., Tooth, S., Duller, G.A.T., 2014. Late Quaternary climatic changes revealed by luminescence dating, mineral magnetism and diffuse reflectance spectroscopy of river terrace palaeosols: a new form of geoproxy data for the southern African interior, Quaternary Science Reviews 95, 43-59.

Macphail, R.I., Goldberg, P., 2017. Applied Soils and Micromorphology in Archaeology, Cambridge University Press, Cambridge.

Mason, R.J., 1961. The Acheulean Culture in South Africa, South African Archaeological Bulletin 16, 107-110.

Mucina, L., Rutherford, M.C., 2006. The Vegetation of South Africa, Lesotho and Swaziland, South African National Biodiversity Institute, Pretoria.

Newesely, H., 1989. Fossil bone apatite, Applied Geochemistry 4, 233-245.

Piga, G., Santos-Cubedo, A., Brunetti, A., Piccinini, M., Malgosa, A., Napolitano, E., Enzo, S., 2011. A Multi-technique approach by XRD, XRF, FT-IR to characterize the diagenesis of dinosaur bones from Spain, Palaeogeography, Palaeoclimatology, Palaeoecology 310, 92-107.

Scott, L., Neumann, F.H., 2018. Pollen-interpreted palaeoenvironments associated with the Middle and Late Pleistocene peopling of Southern Africa, Quaternary International 495, 169-184.

Soil Classification Working Group, 1991. Soil Classification - a Taxonomic System for South Africa, Department of Agricultural Development, Pretoria.

Stoops, G., 2003. Guidelines for Analysis and Description of Soil and Regolith Thin Sections, Soil Science Society of America, Madison, WI.

Stoops, G., Marcelino, V., Mees, F., 2010. Interpretation of Micromorphological Features of Soils and Regoliths, Elsevier, Amsterdam.

Toffolo, M., Berna, F., 2008. Analisi micromorfologica, FTIR e XRD, in: Gelichi, S., Piuzzi, F., Cianciosi, A. (Eds.), “Sachuidic presso Forni Superiore”. Ricerche archeologiche in un castello della Carnia, Edizioni all'Insegna del Giglio, Florence, pp. 50-55.

Toffolo, M.B., Brink, J.S., Berna, F., 2015. Bone diagenesis at the Florisbad spring site, Free State Province (South Africa): Implications for the taphonomy of the Middle and Late Pleistocene faunal assemblages, Journal of Archaeological Science: Reports 4, 152-163.

Toffolo, M.B., Brink, J.S., van Huyssteen, C., Berna, F., 2017. A microstratigraphic reevaluation of the Florisbad spring site, Free State Province, South Africa: Formation processes and paleoenvironment, Geoarchaeology 32, 456-478.

Tooth, S., McCarthy, T.S., Brandt, D., Hancox, P.J., Morris, R., 2002. Geological controls on the formation of alluvial meanders nd floodplain wetlands: the example of the Klip River, eastern Free State, South Africa, Earth Surface Processes and Landforms 27, 797-815.

Tooth, S., Brandt, D., Hancox, P.J., McCarthy, T.S., 2004. Geological controls on alluvial river behaviour: a comparative study of three rivers on the South African Highveld, Journal of African Earth Sciences 38, 79-97.

van der Marel, H.W., Beutelspacher, H., 1976. Atlas of Infrared Spectroscopy of Clay Minerals and their Admixtures, Elsevier Scientific Publishing Company, Amsterdam.

van Hoepen, E.C.N., 1930. Fossiele perde van Cornelia, O.V.S., Paleontologiese Navorsing van die Nasionale Museum Bloemfontein 2, 1-24.

van Hoepen, E.C.N., 1932a. Voorlopige beskrywing van Vrystaatse soogdiere, Paleontologiese Navorsing van die Nasionale Museum Bloemfontein 2, 63-65.

van Hoepen, E.C.N., 1932b. Die stamlyn van die sebras, Paleontologiese Navorsing van die Nasionale Museum Bloemfontein 2, 25-37.

van Hoepen, E.C.N., 1947. A preliminary description of new Pleistocene mammals of South Africa, Paleontologiese Navorsing van die Nasionale Museum Bloemfontein 7, 103-106.

Vingiani, S., Minieri, L., Livadie, C.A., Di Vito, M.A., Terribile, F., 2018. Pedological investigation of an early Bronze Age site in southern Italy, Geoarchaeology 33, 193-217.

Weiner, S., 2010. Microarchaeology. Beyond the Visible Archaeological Record, Cambridge University Press, New York.

Captions

Figure 1. Map of southern Africa showing the location of Cornelia-Uitzoek.

Figure 2. General view of Cornelia-Uitzoek, looking north.

Figure 3. View of the shale bedrock and basal Banded Gravel Bed, looking north. Note the deep incision cut into bedrock by the river and the erosional boundary between sedimentary units.

Figure 4. View of the Banded Gravel Bed and overlying Mottled Yellow Clay, looking south (scale: 20 cm). The trench cross-cuts the bone bed. Solid line marks the boundary between sedimentary units; dashed line marks the limit of the bone bed; white blocks and square are micromorphology samples discussed in the text. Note faunal material in the section (arrows).

Figure 5. View of the Mottled Yellow Clay and Laminated Orange Clay, looking north. The boundary between sedimentary units roughly coincides with the foot of the donga. Note horizontal laminations in the erosional profiles.

Figure 6. View of the Laminated Orange Clay, looking east. Squares mark micromorphology blocks (trowel: 15 cm).

Figure 7. View of the Laminated Orange Clay and Orange Coarse Gravel, looking south (scale: 20 cm). Note the erosional boundary between sedimentary units and vertical root casts. Square marks a micromorphology block.

Figure 8. View of the Laminated Orange Clay, Orange Coarse Gravel, Dark Grey Clay and Black Turf Soil, looking south (trowel: 15 cm). Note the diffuse boundary between topsoil and Orange Coarse Gravel. Squares mark micromorphology blocks.

Figure 9. Representative FTIR spectra of sediments from Cornelia-Uitzoek.

Figure 10. Photomicrographs of representative thin sections from Cornelia-Uitzoek; all images in plane polarized light, except for D in crossed polarized light. A and B: MYC, fragmented clay crusts embedded within the MYC; C: MYC, rounded shale pellet from bone bed deposit; D: MYC, striated b-fabric (lighter orange stringers) indicative of shrink/swell processes; E and F: MYC, juxtaposed coatings of dark-green and yellow clay, bone bed deposit; G: MYC, Fe-Mn oxides aggregate nodules (arrows) superimposed on clay coatings (pale yellow sediment in void); H: MYC, Fe-Mn oxides coating and hypocoating (red-brown halos) around channel.

Figure 11. Photomicrographs of representative thin sections from Cornelia-Uitzoek; all images in plane polarized light, except for E in crossed polarized light. A: LOC, Fe-Mn oxides impregnative feature on groundmass (darker hue), note the marked boundary; B: LOC, coarse, dense infilling of red clay and silt from overlying layers, caused by a root channel; C: LOC, shale pellets bound by bridges of dark-green and yellow clay coatings; D: LOC, juxtaposed coatings of dark-green and yellow clay; E: OCG, dolerite fragment; F: OCG, orthic (left) and disorthic (right) typic nodules of Fe-Mn oxides; G: OCG, orthic concentric nodule of Fe-Mn oxides (arrow); H: BTS, ellipsoid excrements deposited by mites (brown rounded dots).

Figure 12. General view of the donga, looking north. Note the numerous vertical root casts that run through the Orange Coarse Gravel and Laminated Orange Clay. In the latter, cross-sections of the casts are visible from the surface (profile in the background).

Figure 13. Pebbles of shale and dolerite coated with Fe-Mn oxides that formed at the boundary between BTS and OCG. These components are a lag deposit produced by the erosion of BTS and OCG during donga advancement (scale: 20 cm).

Figure 14. View of the topsoil, looking east. Areas that lost plant cover due to donga advancement (arrows) appear dark grey in color due to the oxidation of organic matter in BTS. This deposit occurs in patches at the edge of the donga and was named Dark Grey Clay by Brink et al. (2012).

Figure 15. General view of the donga, looking east. Note channeling caused by water erosion (arrows).

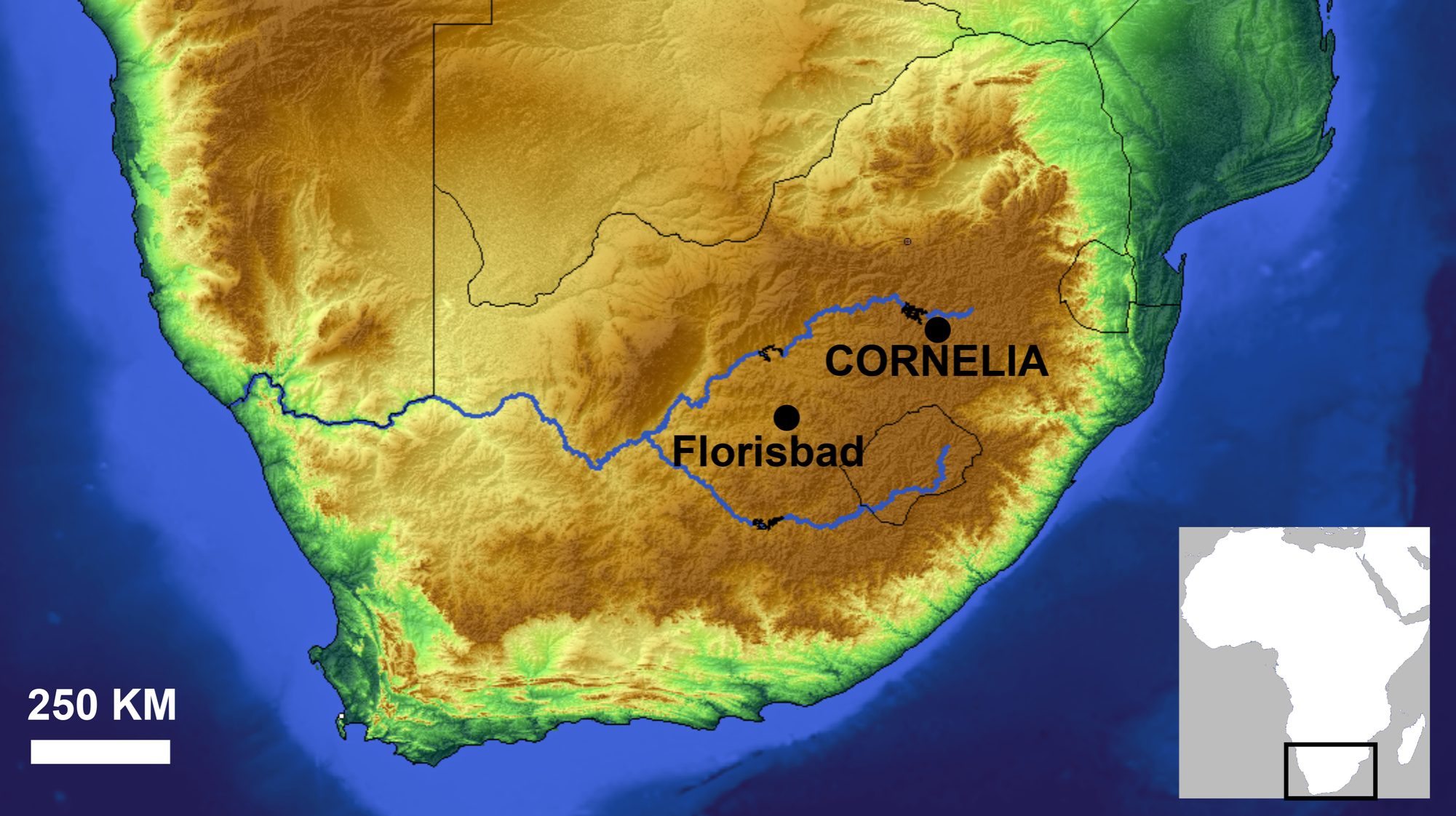
CORNELIA
Florisbad
250 KM

Bone bed
Valley fill and donga

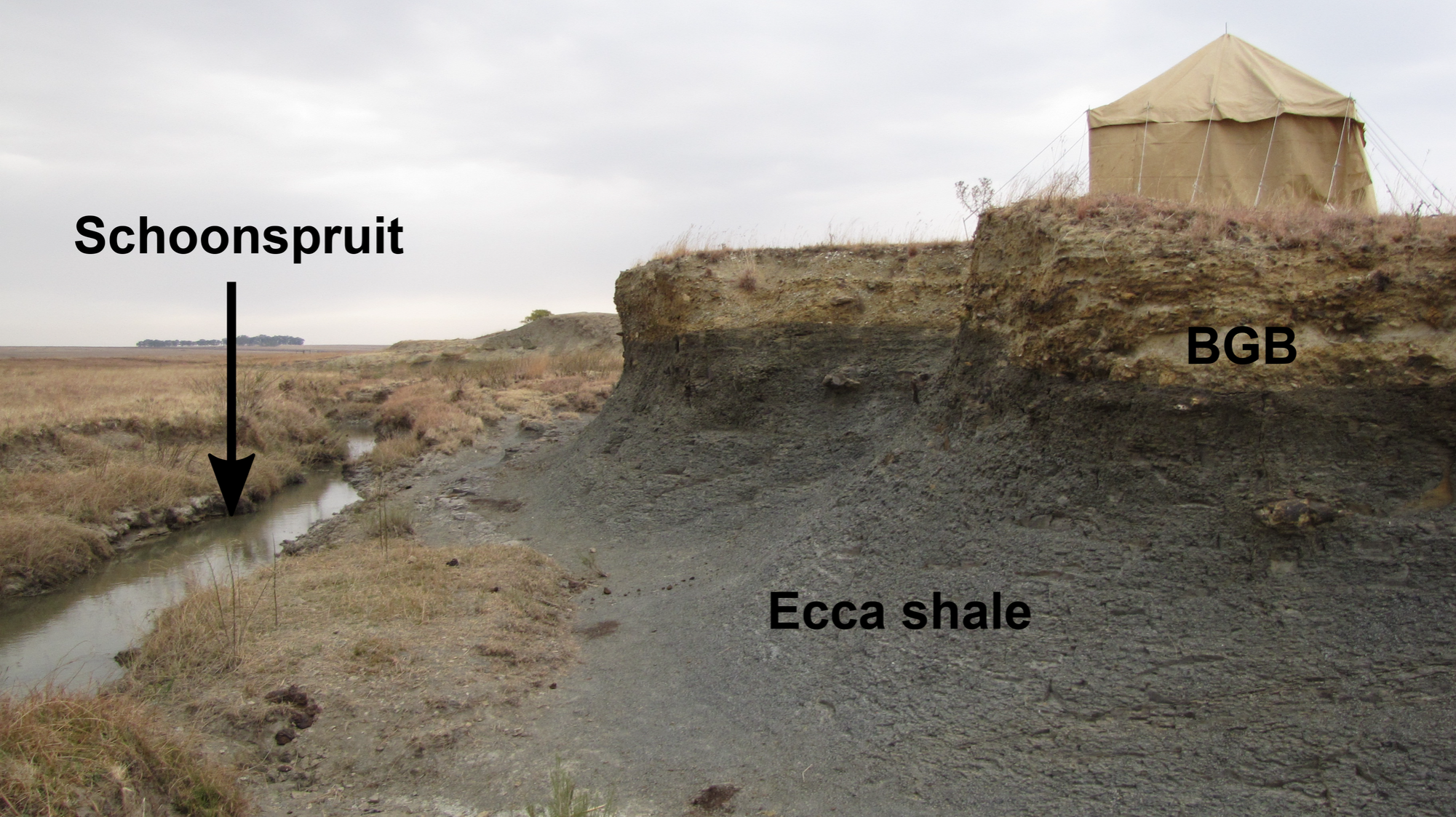
Schoonspruit
BGB
Ecca shale

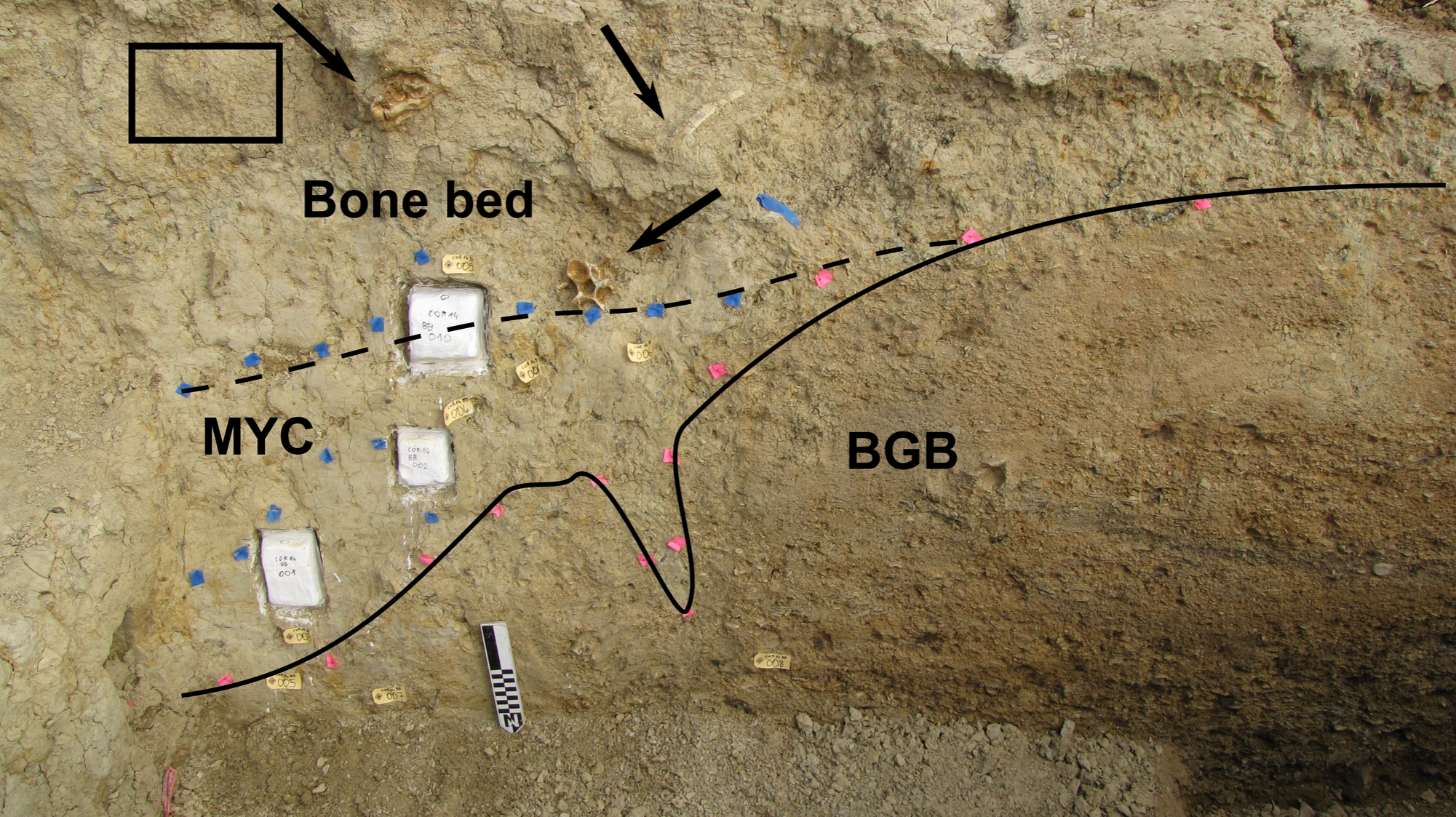
Bone bed
MYC
BGB

LOC
MYC

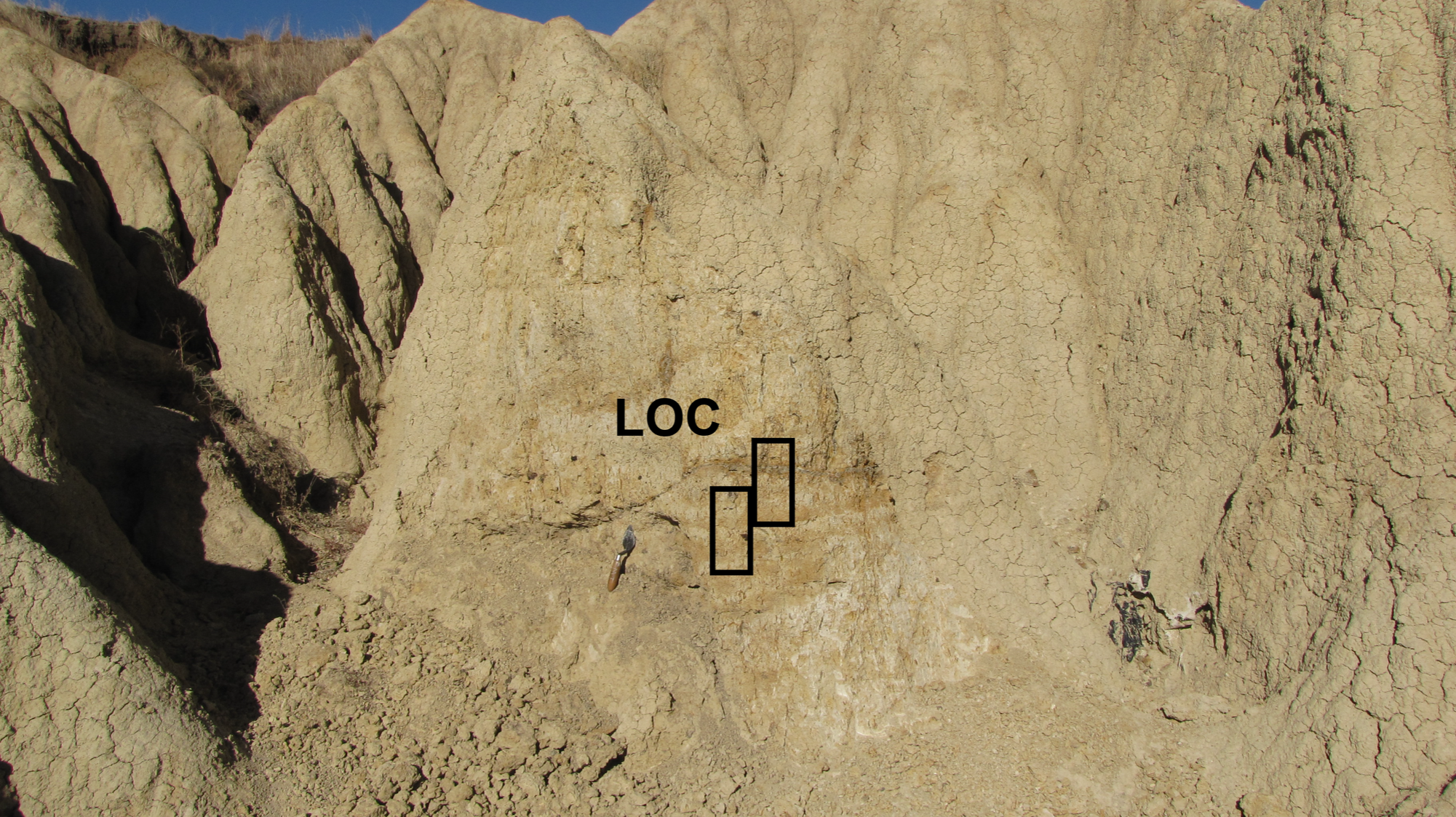
LOC

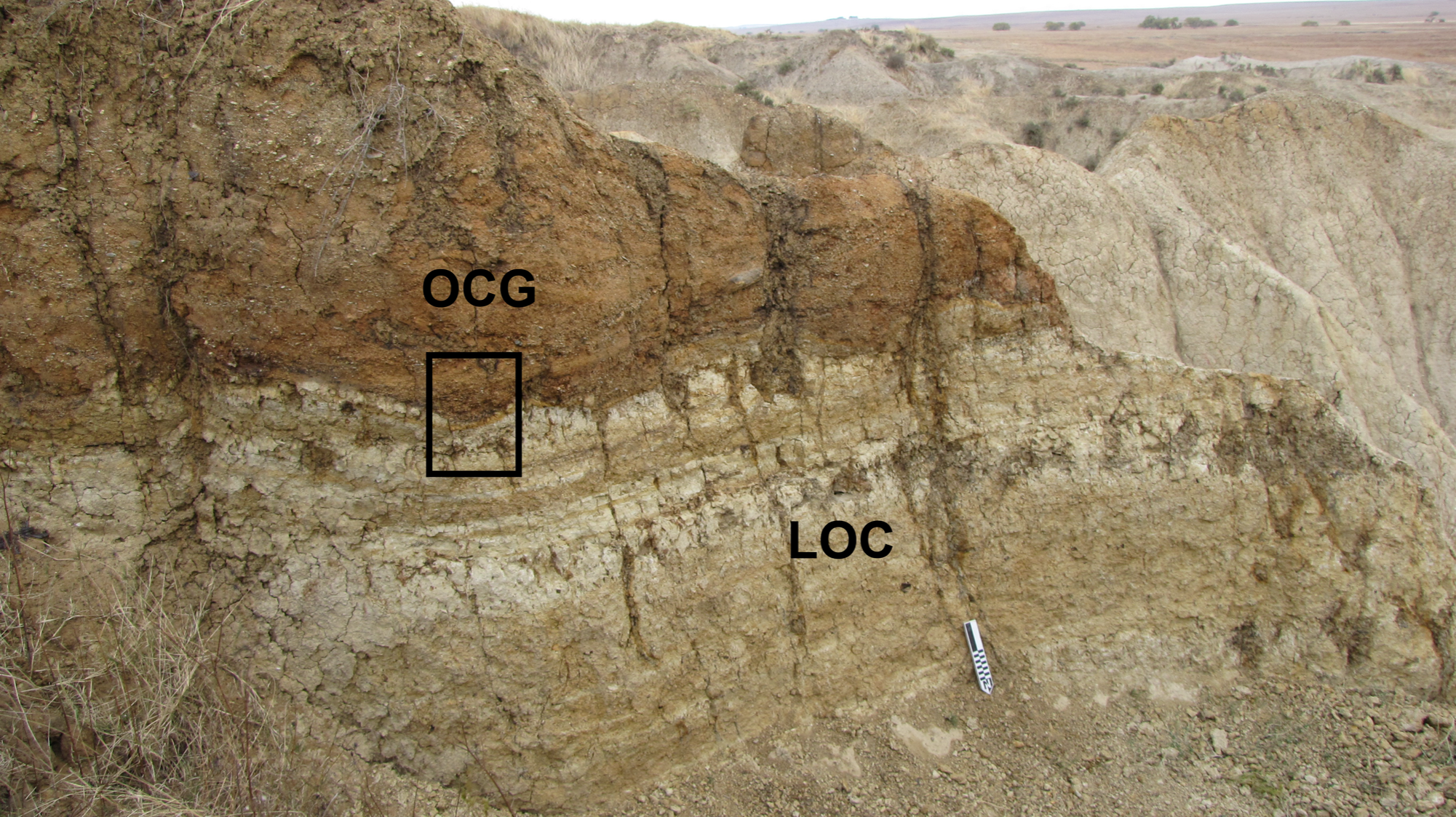
OCG
LOC

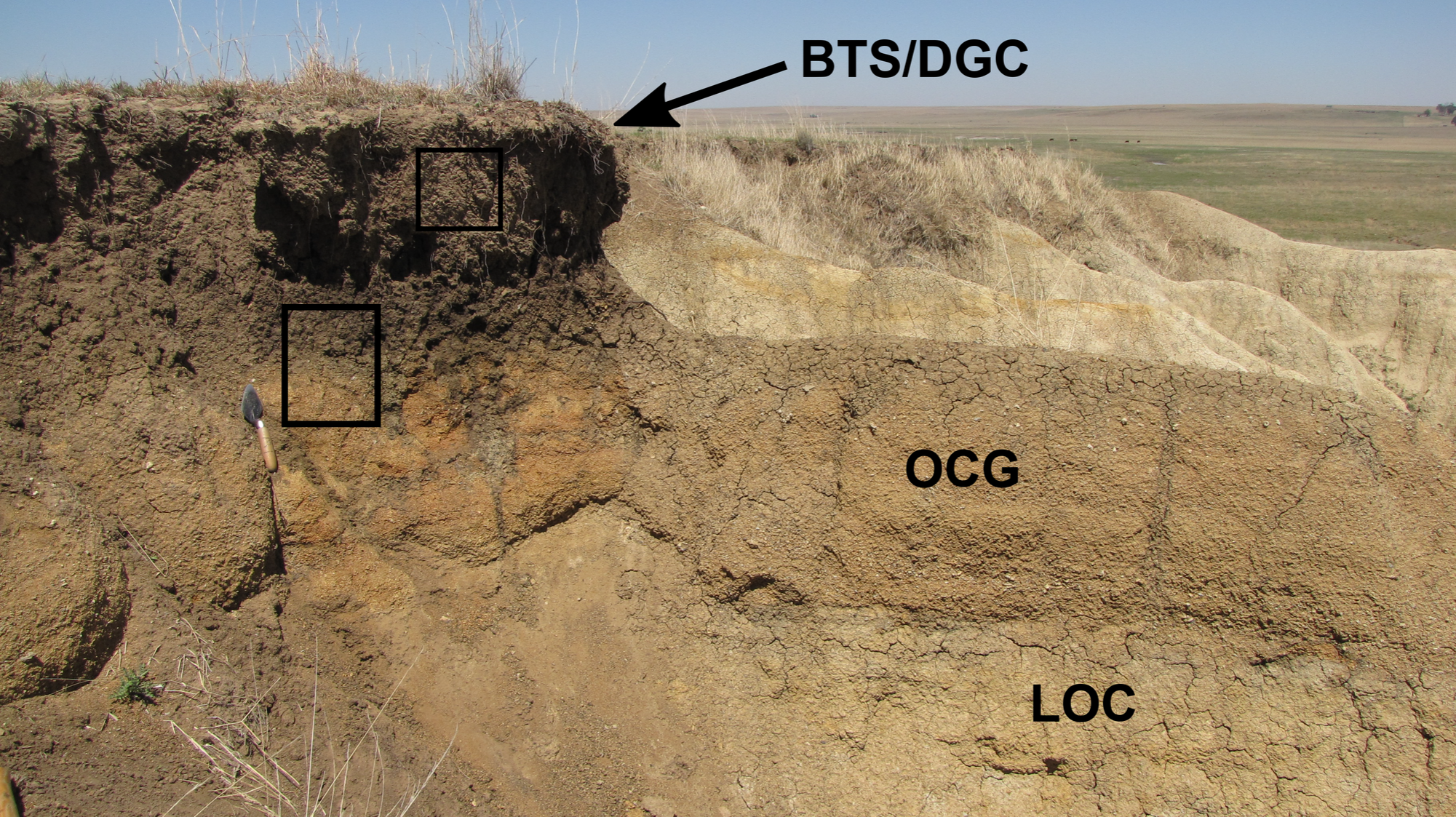
BTS/DGC
OCG
LOC

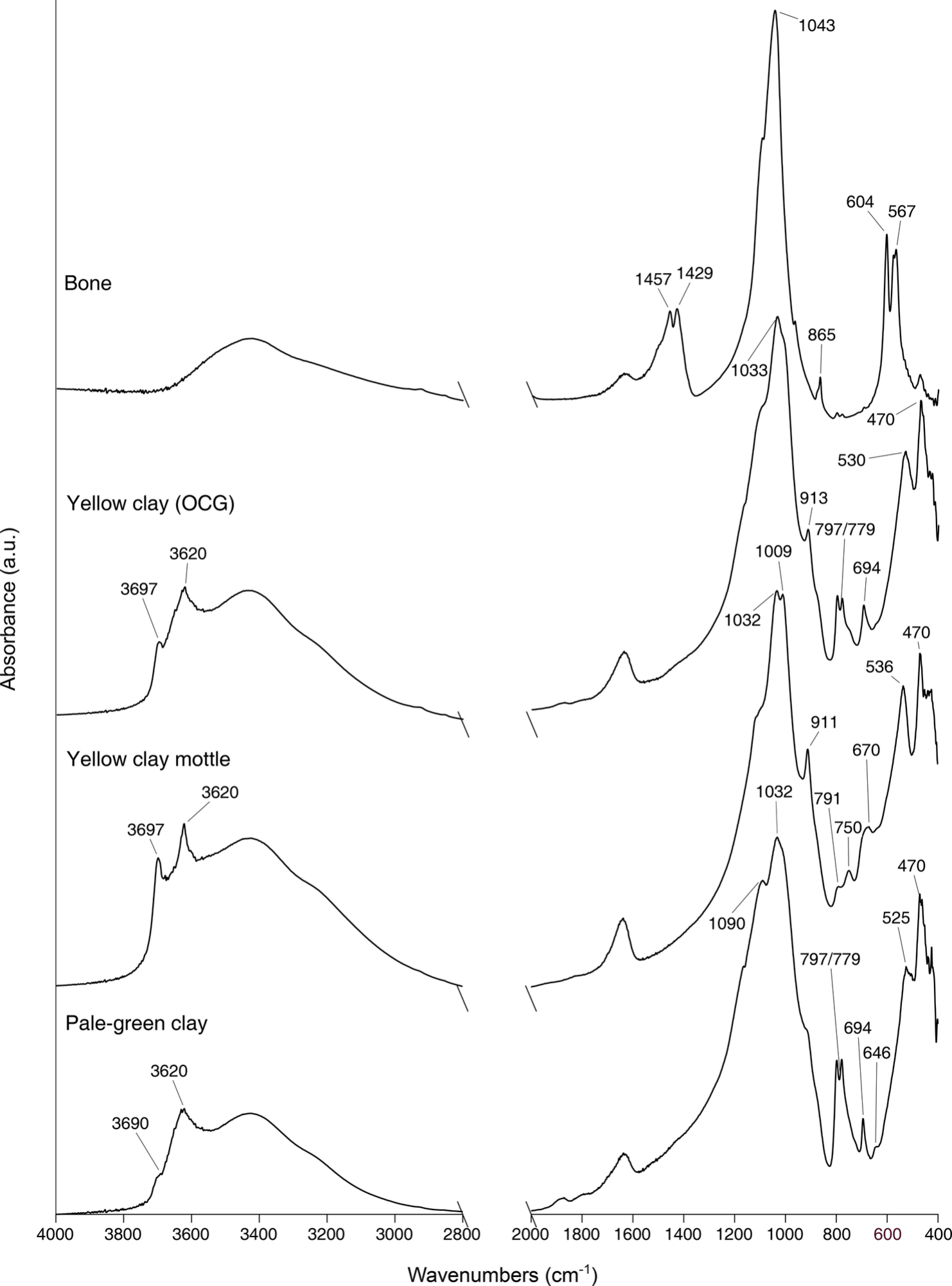
Bone
Yellow clay (OCG)
Yellow clay mottle
Pale-green clay
Absorbance (a.u.)
Wavenumbers (cm-1)
1043
604
567
1457
1429
865
1033
470
530
913
797/779
694
1009
1032
536
911
670
791
750
1090
525
646
3697
3620
3690
4000
3800
3600
3400
3200
3000
2800
2000
1800
1600
1400
1200
1000
800
600
400

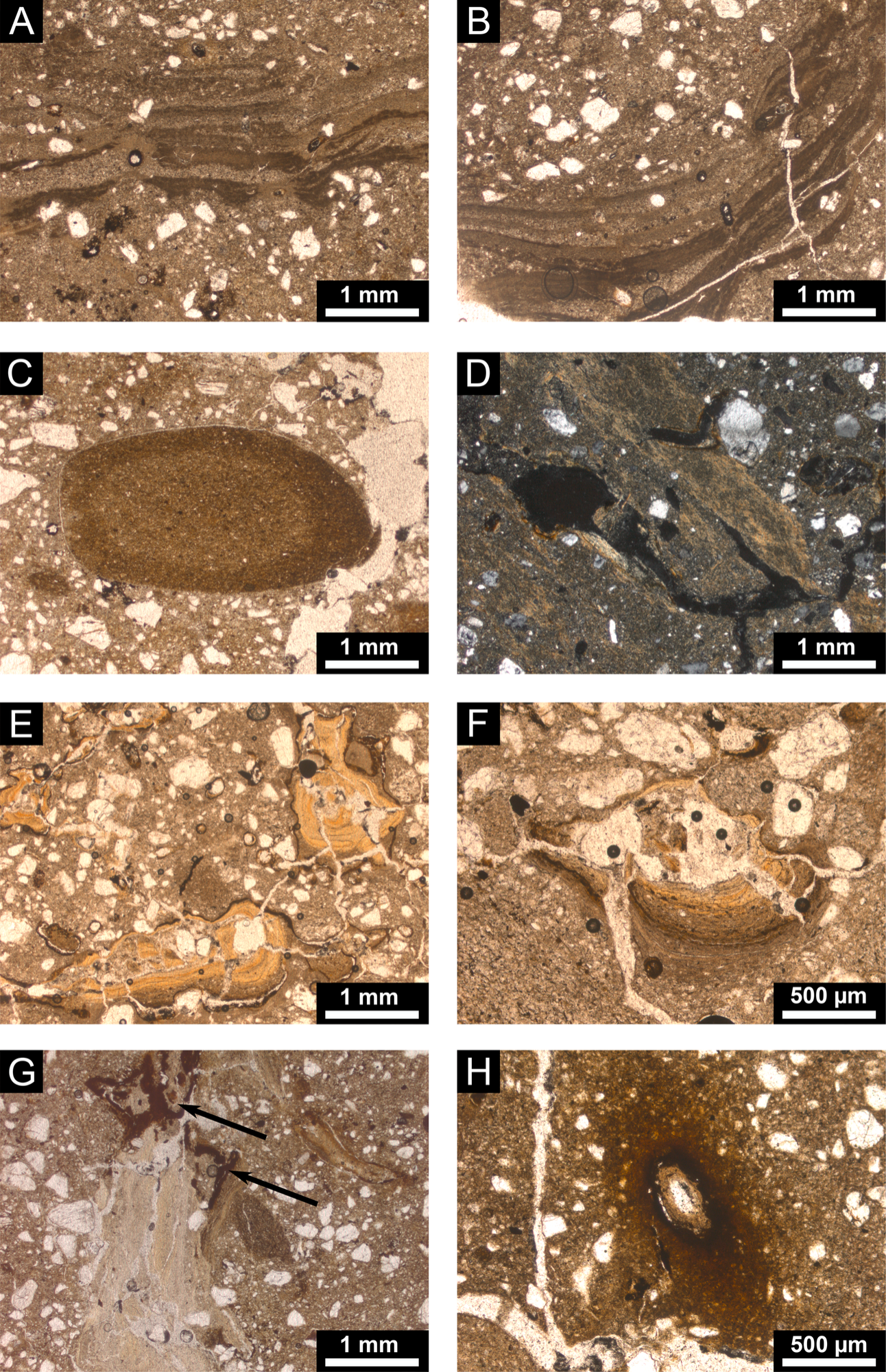
A
1 mm
B
1 mm
C
1 mm
D
1 mm
E
1 mm
F
500 µm
G
1 mm
H
500 µm

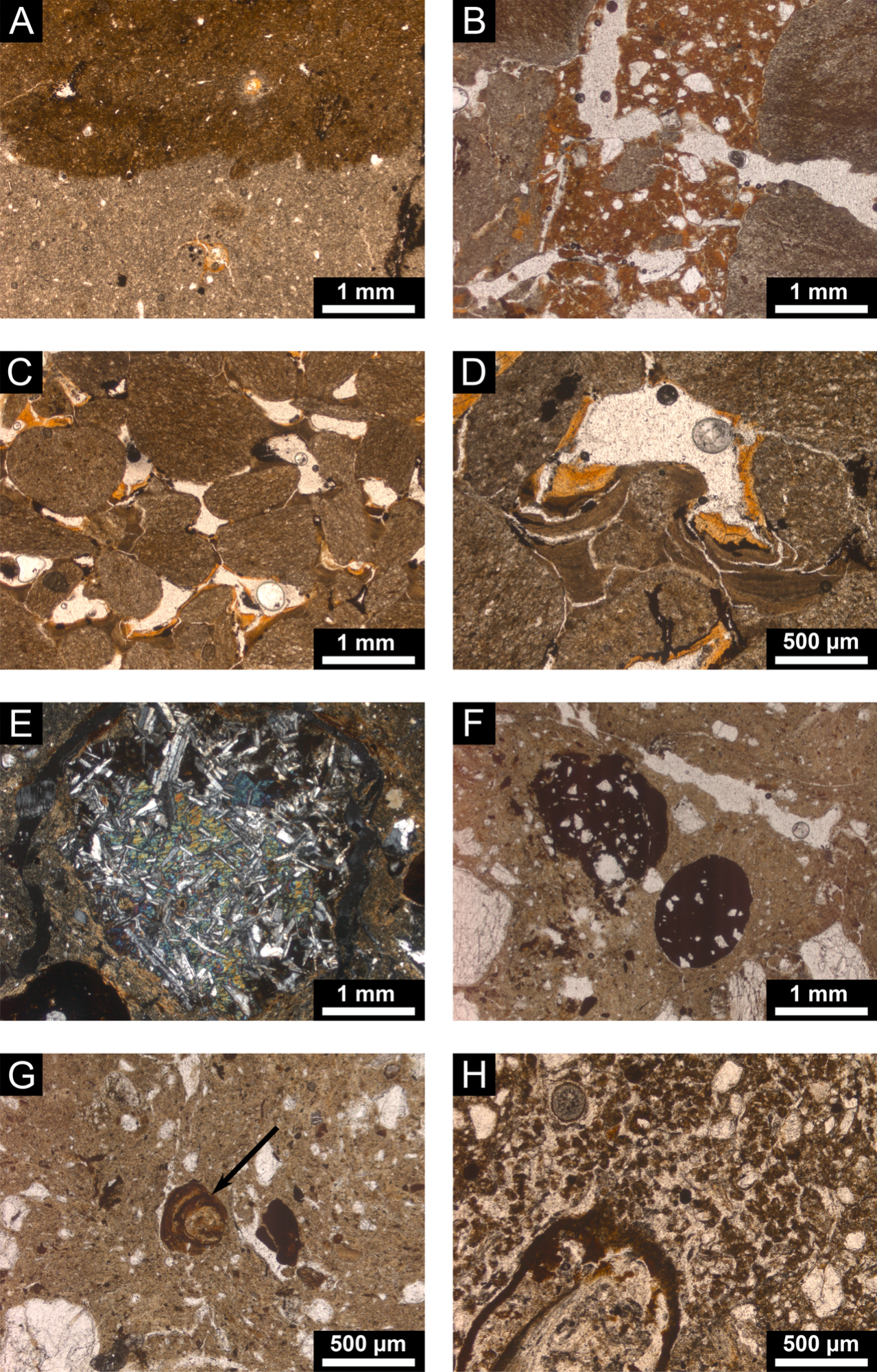
A
1 mm
B
1 mm
C
1 mm
D
500 µm
E
1 mm
F
1 mm
G
500 µm
H
500 µm

N

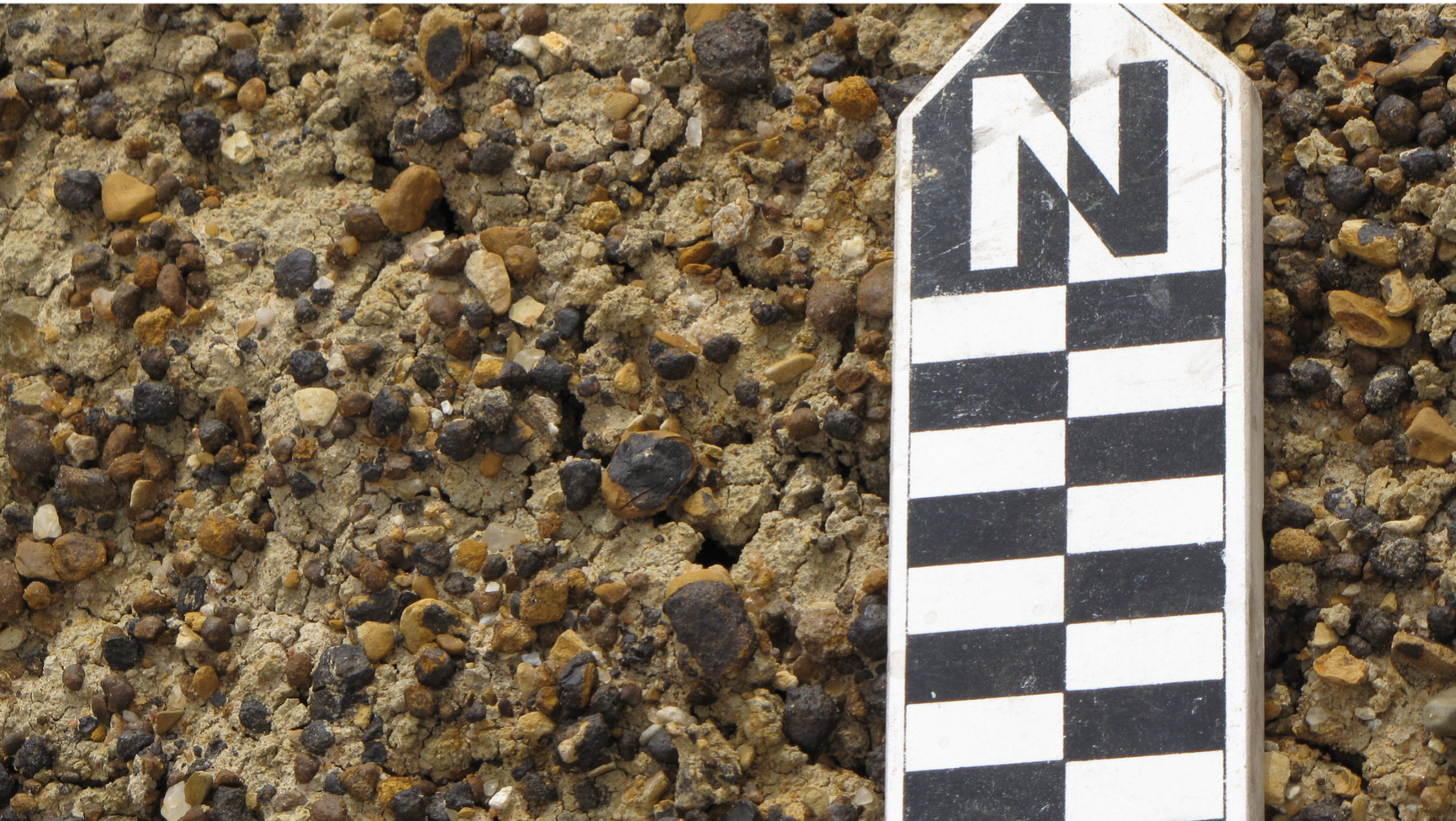
N

DGC

Table 1. Sedimentary units identified at Cornelia-Uitzoek from top to bottom, including data from Brink et al. (2012). Ages are based on paleomagnetism.

Unit	Description	Age (Ma)
Black Turf Soil (BTS)	Topsoil composed of dark brown clay, about 50 cm thick; it contains Middle Stone Age artifacts in places	<0.78
Dark Grey Clay (DGC)	Layer composed of dark grey clay, about 50 cm thick, contiguous to BTS; it contains younger Acheulean artifacts	<0.78
Orange Coarse Gravel (OCG)	Layer composed of gravel, up to 2 m thick at some locations	<0.78
Laminated Orange Clay (LOC)	Layer composed of alternating beds of clay and fine gravel, 2 m thick; it contains small clusters of bones	0.99-0.78
Mottled Yellow Clay (MYC)	Layer of massive pale-yellow to pale-green clay, 3 m thick; it contains a bone bed accumulated by hyenas and Acheulean artifacts	1.07-0.99
Banded Gravel Bed (BGB)	Layer of gravel characterized by normal graded bedding, 1 m thick	>1.07

Table 2. Microfacies types (MFT) identified at Cornelia-Uitzoek. The terminology follows Stoops (2003). MFTs as defined by Flügel (2004).

MFT name	Description	Formation process	Layer
Clay	**c/f related distribution:** close porphyric to open porphyric. **Structure and voids:** weakly to moderately separated angular blocky microstructure with planes and few channels. **Coarse fraction:** sub-angular, silt-sized quartz and feldspar grains (dominant); sub-rounded to sub-angular, medium sand- to very fine sand-sized quartz and feldspar grains (common); rounded, coarse sand- to very fine pebble-sized shale pellets (few). **Fine fraction:** pale-green clay with stipple speckled b-fabric, and in places monostriated, cross-striated, porostriated and granostriated b-fabric. **Pedofeatures:** dusty dark-green clay coatings on voids with striated b-fabric; dusty dark-green clay intercalations with striated b-fabric; limpid yellow clay laminated coatings on voids with striated b-fabric; limpid yellow clay dense infillings with striated b-fabric; moderately to strongly impregnated Fe-Mn oxide orthic aggregate nodules in groundmass, shale pellets and clay coatings/infillings; Fe-Mn oxide hypocoatings and quasicoatings on voids; dark-green clay crusts with striated b-fabric; red silty clay dense infillings with stipple speckled b-fabric; limpid red clay laminated coatings on voids with striated b-fabric.	Overbank deposit (meandering river), shrink/swell, fine and coarse illuviation	MYC, LOC
Fine gravel	**c/f related distribution:** chitonic to concave gefuric. **Structure and voids:** weakly separated granular microstructure to vughy microstructure, with compound packing voids, regular vughs and star-shaped vughs. **Coarse fraction:** rounded, coarse sand- to medium pebble-sized shale pellets (very dominant); sub-rounded, medium sand-sized quartz grains (very few). **Fine fraction:** pale-green clay with stipple speckled b-fabric, and in places granostriated b-fabric. **Pedofeatures:** dusty dark-green clay coatings on voids with striated b-fabric; limpid yellow clay laminated coatings on voids and shale pellets with striated b-fabric; limpid yellow clay dense infillings with striated b-fabric; moderately to strongly impregnated Fe-Mn oxide orthic aggregate nodules in groundmass, shale pellets and clay coatings/infillings; Fe-Mn oxide hypocoatings of voids.	Overbank deposit (meandering river), shrink/swell, fine illuviation	LOC
Coarse gravel	**c/f related distribution:** close porphyric to open porphyric. **Structure and voids:** weakly to moderately separated angular blocky microstructure with planes and few channels. **Coarse fraction:** sub-angular, silt-sized quartz and feldspar grains (frequent); sub-angular to sub-rounded, medium sand- to very fine sand-sized quartz and feldspar grains (frequent); rounded, coarse sand- to very coarse pebble-sized dolerite fragments (few); rounded, coarse sand- to pebble-sized shale pellets (few); elongated fragments of plant tissue (very few). **Fine fraction:** pale-brown clay with random striated, granostriated and porostriated b-fabric. **Pedofeatures:** strongly impregnated Fe-Mn oxide orthic and disorthic typic nodules; weakly impregnated Fe-Mn oxide orthic aggregate nodules on groundmass.	Channel/point bar deposit (meandering river), shrink/swell, eluviation	OCG
Topsoil	**c/f related distribution:** close porphyric. **Structure and voids:** massive microstructure with rare channels. **Coarse fraction:** sub-angular, silt-sized quartz and feldspar grains (dominant); sub-angular to sub-rounded, medium sand- to very fine sand-sized quartz and feldspar grains (common); elongated plant fibers (very few). **Fine fraction:** dark-brown clay with undifferentiated b-fabric; amorphous organic matter. **Pedofeatures:** strongly impregnated Fe-Mn oxide orthic and disorthic typic nodules; spherical and ellipsoid excrements.	Overbank deposit (meandering river), pedogenesis	BTS, DGC